

## APPLICATION OF COMPRESSIVE SENSING TO REFRACTIVITY RETRIEVAL USING NETWORKED WEATHER RADAR

Serkan Ozturk<sup>1,2, \*</sup>, Tian-Y. Yu<sup>1,2</sup>, and Lei Ding<sup>1</sup>

<sup>1</sup>School of Electrical and Computer Engineering, University of Oklahoma, Norman, Oklahoma, USA

<sup>2</sup>Atmospheric Radar Research Center, University of Oklahoma, Norman, Oklahoma, USA

### Abstract

The radar-derived refractivity field can be used as a proxy of near-surface moisture field and has the potential to improve the forecast of convective initialization. The refractivity retrieval was originally developed for the use of single radar, and was recently extended for a network of radars by solving a constrained minimization of mean-square-errors (MSE). In practice, the number of high quality clutter returns can be often fewer than the number of retrieved refractivity points and the retrieval problem becomes ill-defined. In this work, an emerging technology of compressive sensing (CS) is proposed to retrieve refractivity field using a network of radars. It has been shown that CS can provide optimal solution for an underdetermined inverse problem if the conditions of sufficient sparsity and incoherence property are met. For example, CS has been proven to be advantageous over other least mean-square-errors (MSE) based methods if the number of measurements is much fewer than the dimension of signals to be retrieved.

In this work, the relationship between the refractivity field and the phases measured from multiple radars is represented by a linear model. A CS framework with discrete cosine transform (DCT) was used to solve the inversion. The application of CS to refractivity retrieval using single and multiple radars is demonstrated using simulations. In simulation, the model refractivity field was calculated from numerical weather model. Subsequently, the radar-measured phases from randomly located clutterers were generated by integrating refractivity along the ray path. The performance of CS was quantified statistically for various conditions such as the amount of measurement errors, the number of high quality clutter returns, and radar locations. Further, the performance of CS was compared to the method that was developed previously using a MSE approach with smoothness constrain. Our preliminary results have shown that CS can provide relatively robust and high quality estimates of refractivity field for most cases

---

\* Corresponding author address: Serkan Ozturk, University of Oklahoma, School of Meteorology, 120 David L. Boren Blvd., Rm 5340, Norman, OK 73072-7307; e-mail: serkanozturk@ou.edu

### 1. INTRODUCTION

Moisture is one of the critical parameters to improve the forecast of storm initiation in the warm season. Therefore, atmospheric moisture must be measured with high temporal and spatial resolution accuracy that can be used to predict exact timing and location of convective initiation [14]. However, high resolution observations of the moisture field are often limited.

It has been known that refractivity is directly affected by atmospheric parameters which are pressure, temperature, and moisture. A technique was developed to estimate refractivity by exploiting the phase of radar signals from ground clutter using single radar [8] since refractivity is closely tied to the moisture at warm temperature [1]. It has been suggested that refractivity measured by weather radar can be used as a proxy for near-surface moisture field. Observations using weather radar for near-surface moisture are available per scan approximately a few minutes and a few kilometers. Low level-atmospheric refractivity can be represented by radar-derived refractivity retrieval.

Since the refractivity is a function of temperature and humidity, the phase change of radar's signals from stationary ground targets depend on the refractivity along the path. Radar-derived refractivity retrieval is implemented on several research with S, X, C bands operational radar and feasibility of refractivity retrieval has been demonstrated in several field [13], [12].

The rapid refractivity retrieval algorithm was developed for single radar phase measurements from ground clutterers by performing a range derivative operation. Then, it was demonstrated and investigated using the phased array radar at National Weather Radar Testbed (NVRT) [5]. The radar derived refractivity application to mesoscale and storm scale weather phenomena surveyed and analyzed to study in [3], [2]. It was shown that the radar derived refractivity has a good agreement with surface measurements and so provide sufficient operational forecast [14]. Recently, the refractivity retrieval field estimation model using network weather radar was derived and verified with simulations and with real data [10], [9].

The phase measurements from refractivity field are indi-

cated by a linear model using gridded approach. Therefore, the estimation of refractivity from these measurements was assumed as an inversion problem and solved by using constrained least square (CLS) method.

In this work, compressive sensing (CS) technique [4], [7] is used to reconstruct the refractivity from the phase measurements by designing the same linear model. The number of pixels on the rectangular linear map which is refractivity reconstructed is much higher than the number of measurements. Therefore, the linear model becomes underdetermined set of linear equations [10]. We demonstrated that the two conditions of sparsity and incoherency, required by the CS, are likely to be met for the problem of refractivity retrieval. It has been shown that CS can provide reliable and effective recovery for underdetermined cases.

The remainder of this paper is organized as follows. In section 2, formulation of refractivity retrieval with networked radar will be briefly reviewed. A review of proposed compressive sensing algorithm in section 3 and refractivity estimation using CS and CLS in section 4. refractivity simulation with demonstration of results in section 5. Statistical analysis of CS and CLS algorithms with results will be in section 6. The summary is presented in section 7.

## 2. FORMULATION OF REFRACTIVITY RETRIEVAL WITH NETWORKED RADAR

It is well known that refractivity is closely tied to meteorological parameters and becomes more depended on the relative humidity as temperature increases [5] at a surface pressure which is considered as a constant. Given a stationary target located at range of  $R$  from the radar, the phase of radar signal depends on the integration of refractivity along the ray path. Estimation of refractivity field is made by exploiting phase difference of radar signals from a stationary ground target at two different time of observations. In this work, we focused on the refractivity changes ( $\delta N$ ) from consecutive scans. Moreover, we assumed the phase wrapping was dealt with separately. However, a solution was proposed to avoid from phase wrapping and unwrapping issue using the differences in phase between two different times [8].

The refractivity estimation algorithm was proposed for multiple radars [10] and implemented [9]. In the system, we assumed that there are  $J$  stationary targets with  $K$  radars in the measurement field, then the number of measurement is  $L = KJ$ . Then, all the phase differences can be formed in a measurement vector with size of  $L$  by 1. When the number of targets are high enough, then the probability of the crossing  $L$  paths in the field will be

high and so the refractivity field can be reconstructed with high probability.

It is assumed that refractivity field is parameterized with a finite set of variables and the measurement field is gridded into  $M \times N$  pixels ( $MN=P$ ) and since the refractivity field is continuous, refractivity index value in each pixel is divided by  $10 \times 10$  sub-squares and assumed to be a constant. Eventually, using this gridded approach with finite dimension, the measurement of phase differences are represented in a linear model [10].

$$\Phi = H\eta + e \quad (1)$$

where  $\Phi$  is a column vector of measured phase differences with a size of  $L$  by 1,  $\eta$  is a column vector form of refractivity difference  $\delta N$  with a size of  $P$  by 1,  $H$  is linear operator to represent the path-integrated measurement with size of  $L$  by  $P$ , and  $e$  is the measurement errors with size of  $P$  by 1.

The measurements are vertically ordered in the measurement vector based on the path integration sequence. Measurement matrix ( $H$ ) is obtained by using ray path-integrated over the field in a linear form. Note that each row has only one measurement coefficients and it is in a linear model which can be applied to single radar case ( $K=1$ ). On the other hand, the number of measurements decrease compared to a multi-radar case for the same number of targets. The refractivity field estimation discussed for single radar in [8], [5] using different approach and for multi-radar in [10] using constraints.

The phase measurement was defined in a linear form with the refractivity changes in equation (1). Now, the refractivity retrieval  $\eta$  is to estimate from  $\Phi$  with  $L$  measurement. In general sense,  $L$  is much smaller than  $P$  and so the  $H$  matrix is sparse, it is ill-posed condition. Hence, direct inverse of  $H$  matrix is not exist and the direct least square solution cannot be applied. A constrained optimization method was used to solve this problem [10]. On the other hand, for both single and networked radars cases, CLS can be applied to solve the underdetermined inverse problem of (1) by including a smoothing constraint. In this work, the compressive sensing technique is applied to solve the inverse problem to recover refractivity with the goal of robust estimation.

## 3. PROPOSED ALGORITHM CS

Mathematical theory of compressive sensing (CS) has been studied in the literature of Information Theory and Approximation Theory as an abstract general setting [4], [7] and it is successfully applied to rapid MRI imaging

and its details were presented [11].

In most cases, a signal or image can be reconstructed using much less number of measurements comparing to nominal number of measurements are needed. Therefore, CS relies on two principles that are sparsity and incoherence. CS can provide an optimum and unique solution using nonlinear L1 norm if the refractivity field is sparse and incoherent with the measurement basis. On the other hand, most of finite dimensional signals are compressible in its original domain or a known transform domain  $\Psi$ . That is, a signal can be expressed with sparse transform coefficients in the proper basis and number of transform coefficients are relatively small against to nonzero values.

Hence, refractivity fields must have a sparse representation in the proper transform domain to be reconstructed. These two conditions for refractivity retrieval are discussed in the following. The sparsity can be achieved in the image domain or after a transformation. In this work, the discrete cosine transform (DCT) was used and can provide promising results. So, we have the discretized model with gridded array of  $P$  pixels ( $M \times N$  dimension) and refractivity can be written as

$$\boldsymbol{\eta} = \boldsymbol{\Psi}\mathbf{x} \quad (2)$$

where  $\boldsymbol{\Psi}$  is orthonormal basis (such as DCT) and has  $P \times P$  dimension matrix with  $\psi_1, \dots, \psi_P$  as columns.  $\boldsymbol{\eta}$  is vectored form of the pixels with size of  $P \times 1$  and  $\mathbf{x}$  is the transform coefficients of the DCT with  $S$  largest nonzero values.

Figure 1 demonstrates that the model reflectivity change can be represented reasonably well by using only 103 significant coefficients out of 4096 coefficients, which suggests that the refractivity field is sparse in the DCT domain. In Figure 1, the model field of refractivity changes is shown on the left panel with 4096 pixels (64 by 64 km with a 1 km grid spacing) and the first 150 DCT transformation coefficients are shown in the middle panel after sorting. The refractivity obtained by the inverse DCT using the largest 103 significant coefficients is shown is on the right panel. It is evident that the image can be represented well by using only 2.51 % of the coefficients.

In other words, only 2.71 % of the coefficients are sufficient to represent the model refractivity. Incoherence gives the relationship between sampling measurement basis  $H$  and sparse representation basis  $\boldsymbol{\Psi}$ . In other words, incoherence measures the the smallest correlation between any two elements of  $H$  and  $\boldsymbol{\Psi}$ . The coherence pairs between the transformation basis and measurement basis is defined in the following equation

$$\mu(H, \boldsymbol{\Psi}) = \sqrt{P} \max(|\langle H_i, \psi_j \rangle|) \quad 1 \leq i, j \leq P \quad (3)$$

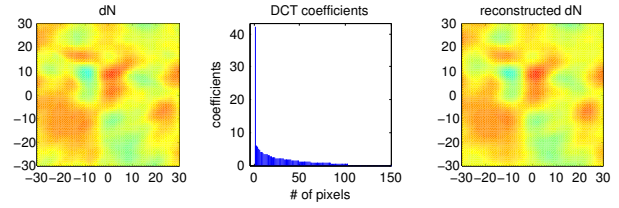


Figure 1: The model field of refractivity changes is shown on the left panel with 4096 pixels (64 by 64 km with a 1 km grid spacing) and the first 150 DCT transformation coefficients are shown in the middle panel after sorting. The refractivity obtained by the inverse DCT using the largest 103 significant coefficients is shown is on the right panel. It is evident that the image can be represented well by using only 2.51 % of the coefficients

The coherence will be large when the pair of  $(H, \boldsymbol{\Psi})$  includes correlated elements, otherwise it will be small. The range of coherence is  $[1, \sqrt{P}]$ . CS requires the coherence as low as possible within a given range. For our case, the coherence between the measurement basis of  $H$  from the target distribution in Figure 1 and the DCT transformation is 11.308 given the range between 1 and 64. This suggest that the DCT transform can provide low coherence with the measurement matrix.

Moreover, it must be avoided that the samples from linear combinations are not focused on a few sparse coefficients. In this work, CS is applied to estimate refractivity field from linear combinations of measurement which are the integral of the refractivity differences along each path between radar and targets. We expect in this framework that CS seems to be able to make accurate recovery of refractivity fields from small subset of phase change measurements with the limited number of targets. We claim that the linear model of the refractivity is met for the CS principles to reconstruct the signal accurately.

#### 4. REFRACTIVITY RECONSTRUCTION

The phase measurements are obtained linearly from the product of the measurement basis against the refractivity. Now, the refractivity is wanted to reconstruct using this linear form that the number of measurements are much less than the number of pixels and so there is no unique solution for this inverse problem and it is highly ill-posed.

$$\boldsymbol{\Phi} = \mathbf{H}\boldsymbol{\eta} + \mathbf{e}, \quad i \in L \text{ and } L < P \quad (4)$$

CS requires nonlinear reconstruction of the refractivity field which is convenient to the CS setting. Moreover,

CS searches the unique solution in the sparse domain using the  $\Psi$  transformation matrix. Because sparse signals have small  $l_1$ -norm value. The nonlinear  $l_1$ -norm reconstruction is obtained by solving the following constraint optimization problem

$$\min \|\Psi' \hat{\eta}\|_1 \quad \text{subject to} \quad \|\Phi - H\hat{\eta}\|_2 < \beta \quad (5)$$

Where  $\beta$  bounds the amount of noise in the phase measurement and usually set below the expected noise level.  $\Psi$  is the matrix operator to get the discrete cosine transform (DCT) of the refractivity images. The threshold level of the sparse representation is selected based on the estimated noise level [6]. Selecting suitable sparse representation helps to achieve a sparseness and incoherence. Thus, the signal is concentrated on randomly and relatively small set in the sparse transformation basis.

The role of  $l_1$ -norm minimization is the most significant feature for the proposed approach. The CS reconstruction is used nonlinear approximation as the measurements are linear. The inverse DCT operator  $\Psi'$  takes an P-point transform of the candidate image  $\hat{\eta}$  and the transform coefficients are obtained in a vector form.  $l_1$ -norm of the vector is only the summation of the magnitudes and it selects the minimum value among the iterations since  $l_1$  norm of sparse signal is often small. The constraint convex optimization problem could be written as unconstraint problem in Lagrangian form

$$\min \|\Phi - H\hat{\eta}\|_2^2 + \theta \|\Psi' \hat{\eta}\|_1 \quad (6)$$

where theta is regularization parameter that determines the trade off between the sparseness and data fidelity. Selecting the parameter theta appropriately, the solution of 5 will be exactly to 3. The non-linear conjugate gradients and backtracking line search [11] is implemented to solve the unconstraint optimization problem.

On the contrary,  $l_2$  norm minimization is generally used for regularization and the large coefficients are penalized severely. Thus,  $l_2$  norm results become over-smooth. Besides, using the regularization, it often needs to apply a smoothness function with reconstruction which is called constraint least square (CLS) technique [10]. In addition, the refractivity field is retrieved using the phase measurement by applying CS and CLS techniques for single radar and networked radars.

## 5. REFRACTIVITY SIMULATION

The application of the CS to refractivity retrieval was implemented for a single radar and networked radars over the simulation domain with size of 64 by 64 km. The

model refractivity fields ( $\eta$ ) were obtained from a numerical weather model from 19-May-2010 from 2000 to 2115 UTC in Oklahoma. The model field varies from -3.98 to 1.34 N units. Subsequently, zero mean Gaussian noises with desirable standard deviation were added to refractivity field in the simulation of radar phase measurements. In CS, the refractivity was estimated from the minimization of the nonlinear  $l_1$  norm of the transformation coefficient subject that the  $l_2$  norm of errors is small.

The first case is designed for a single radar refractivity retrieval that the radar location is on the left at the bottom of the domain (-32, -32) km. Approximately 400 clutter targets are generated randomly on the simulation domain and their locations are denoted by "x" in Figure 2. An example of the model refractivity changes from the numerical weather prediction model is shown on the left panel of Figure 2 and the simulated phase measurements using (1) is shown on the right panel after spatial interpolation.

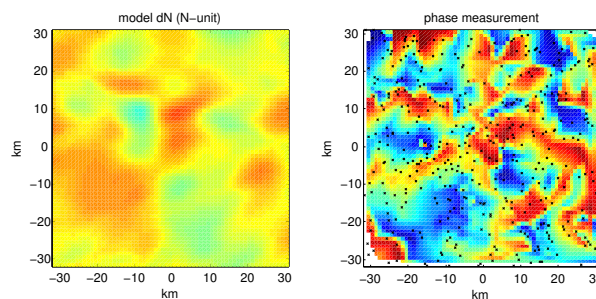


Figure 2: (Left) Refractivity differences and (right) phase measurements using one radar located at (-32, -32) km. The location of 400 ground clutter is denoted by x in the right panel.

For a single radar setup, the refractivity field recovered using CS and CLS techniques with 1N unit noise and the results are shown in Figure 3. The refractivity field was estimated by CLS and CS with 400 phase measurements and 1N-unit error. It is evident that both CS and CLS can grossly reconstruct the refractivity changes by comparing to the model as shown on the left panel of Figure 2. Moreover, CS and CLS reconstructed images with RMSE of 0.17 and 0.24, respectively.

Additionally, it is assumed that the phase wrapping and unwrapping is performed without error for both algorithms. The refractivity is reconstructed using 400 phase measurements within the domain with 1 x 1 km grid resolution for CS and CLS. The measurement ratio of the unknown number of pixels,  $L=400$  and  $P=4096$ , is around 10%.

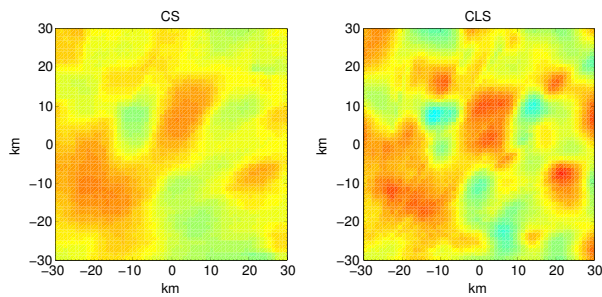


Figure 3: (Left) Refractivity differences and (right) phase measurements using one radar located at (-32, -32) km. The location of 400 ground clutter is denoted by x in the right panel.

The reconstructed refractivity changes using CS and CLS for a network of three radars are shown on the left and right panels of Figure 4. The additional two radars are located at (-32, 32) km and (32, -32) km. It is evident that both CS and CLS provide improved performance using three radars. As the number of radars increases, the number of measurements increases and the number of paths passing through a given pixel is likely to increase. Moreover, CS provides better reconstruction than CLS for this case

It is clearly seen from the Figures using single and net-

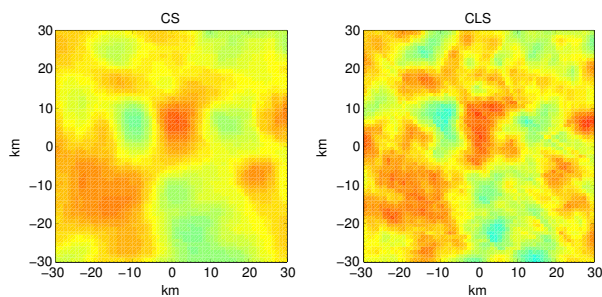


Figure 4: The refractivity retrieved by CLS (left panel) and CS (right panel) using 3 radars and 400 ground clutters with 0.5 N unit error. The radars are located at the left and right lower corners and at the top left. Increasing the number of radars, the number of measurements and crossing paths are increased.

worked radars that both techniques can recover the  $\delta N$  field that is consistent with the model. CS refractivity retrieval performs better than CLS against noisy and has better suppression for the noise. CLS is more sensitive to noise than CS and so the reconstructed refractivity field from CLS is more noisy. Both algorithms have a more error on the boundary of the domain and for the fair comparison the edges at the boundary are omitted. The root mean square error (RMSE) is used to analyze

the performance of algorithms.

$$RMSE = \sqrt{\frac{1}{P} \sum_{i=3}^M \sum_{j=3}^N [\delta N(i, j) - \delta \hat{N}(i, j)]^2} \quad (7)$$

where  $\delta \hat{N}$  is reconstructed refractivity change and  $M=N=62$  is the number of pixels in one direction, and  $P=MN$  as total number of pixels. Since the fair comparison, two rows and columns of edges were omitted from four side of the reconstruction and so the RMSE calculation is start  $i=j=3$  to 62. As a result, the RMSE of CS and CLS is 0.15 and 0.27, respectively.

## 6. STATISTICAL ANALYSIS

In order to investigate robustness of the CS and CLS, various amount of noise were added to the model. For statistical analysis, 20 realizations were performed for each given radar configurations (1-3 radars), amount of noise, and number of measurements. Root mean square error (RMSE) between the reconstructed and the model were used to compare the performance of the CS and CLS.

The mean and SD of the RMSE from CS and CLS as a function of amount of noise are shown in Figure 5 for 1, 2, and 3 radars configurations. The number of phase measurements was obtained from 400 ground clutters with a good quality. In order to make a fair comparison due to the boundary problems, 94 % of the images are used to compare.

For single radar and no noise case, CS has slightly

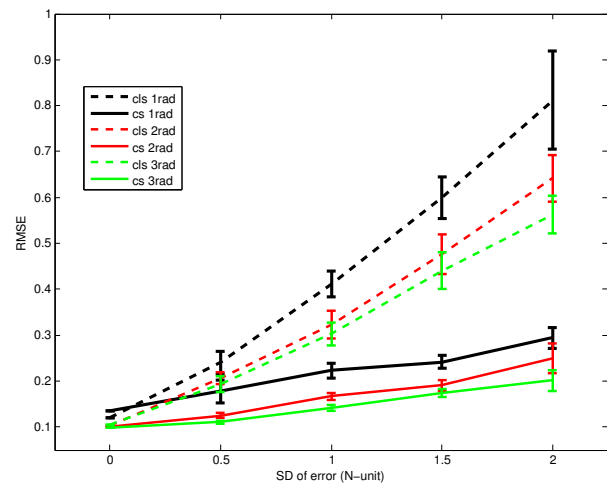


Figure 5: The mean and SD of RMSE from the CS (solid line) and CLS (dash line) versus N-unit errors using single radar and networked radars with 400 targets.

higher RMSE than CLS. However, if noise is considered, CS has the lowest RMSE and small SD of variations for all the different amounts of noise. CLS has the highest SD of RMSE for 2 N-unit error but CS has more stable. The slope of CS is much lower than CLS between no noise and 0.5 N-unit error and also, for other cases. For networked radars, CLS and CS have quite similar RMSE for no noise case. However, when noise was added, CLS produce more noise results and so the RMSE become much higher than CS. The slope of CS is more lower and SD of CS is much stable than CLS. Both algorithms have the lowest RMSE for 3 radars configuration, as comparing the other two configurations. SD and mean of the RMSE decrease as increasing the number of radars since the number of measurement and crossing the number of pixels increase simultaneously.

## 7. SUMMARY

In this work, the applications of CS to refractivity retrieval was demonstrated using numerical simulation for a single radar and networked radars. Performance of CS and CLS was evaluated statistically and compared using RMSE. It is evident that CS and CLS can reconstruct the refractivity field consistently, while CS has the best performance with the lowest RMSE for all the three radar configurations and noisy cases. The results also suggest that CS is less susceptible to noise compared to CLS.

## ACKNOWLEDGEMENT

This work was primarily supported by the National Science Foundation (NSF) ATM0750790.

## References

- [1] Bodine, D., P. Heinselman, B. L. Cheong, R. D. Palmer, and D. Michaud, 2008: Convection initiation and storm evolution forecasting using radar refractivity retrievals. in *24th Conf. on Severe Local Storms*.
- [2] Bodine, D., P. L. Heinselman, B. L. Cheong, R. D. Palmer, and D. Michaud, 2010: A case study on the impact of moisture variability on convective initiation using radar refractivity retrievals. *J. Appl. Meteor.*, **49(8)**, 1766–1778.
- [3] Bodine, D., P. L. Heinselman, R. D. Palmer, B. L. Cheong, and D. Michaud, 2009: Survey of applications of radar refractivity retrievals. *Amer. Meteor. Soc.*
- [4] Cands, E. J., J. Romberg, and T. Tao, 2006: Robust uncertainty principles: exact signal reconstruction from highly incomplete frequency information. *IEEE Trans. Inform. Theory*, **52**, 489–509.
- [5] Cheong, B. L., R. D. Palmer, C. Curtis, T.-Y. Yu, D. Zrnic, and D. Forsyth, 2008: Refractivity retrieval using the phased array radar: First results and potential for multi-function operation. *IEEE Trans. Geosci. Remote Sens.*, **46(9)**, 2527–2537.
- [6] Ding, L., 2009: Reconstructing cortical current density by exploring sparseness in the transform domain. *Physics in Medicine and Biology*, **54**, 2683–2697.
- [7] Donoho, D., 2006: Compressed sensing. *IEEE Trans. Inform. Theory*, **52**, 1289–1306.
- [8] Fabry, F., C. Frush, I. Zawadzki, and A. Kilambi, 1997: On the extraction of near-surface index of refraction using radar phase measurements from ground targets. *J. Atmos. Oceanic Technol.*, **14**, 978–987.
- [9] Fritz, J., and V. Chandrasekar, 2009: Implementation and analysis of networked radar refractivity retrieval. *J. Atmos. Oceanic Technol.*, **26**, 2123–2135.
- [10] Hao, Y., D. Goeckel, R. Janawamy, and S. Frasier, 2006: Surface refractive index field estimation from multiple radars. Vol. 41, pp. RS3002, doi:10.1029/2005RS003288.
- [11] Lustig, M., D. Donoho, and J. M. Pauly, 2007: Sparse MRI: The application of compressed sensing for rapid MRI imaging. *Magn Reson Med*, **58**, 1182–1195.
- [12] Roberts, R., F. Fabry, P. Kennedy, E. Nelson, J. Wilson, N. Rehak, J. Fritz, V. Chandrasekar, J. Braun, J. Sun, S. Ellis, S. Reising, T. Crum, L. Mooney, and B. Palmer, 2008: Refract-2006: Real-time retrieval of high-resolution, low-level moisture fields from operational NEXRAD and research radars. *Bull. Amer. Meteor. Soc.*, **89**, 1535–1548.
- [13] Weckwerth, T. M., D. B. Parsons, S. E. K. J. A. Moore, M. A. LeMone, B. B. Demoz, C. Flamant, B. Geerts, J. Wang, and W. F. Feltz, 2004: An overview of the international h2o project (ihop-2002) and some preliminary highlights. *Bull. Amer. Meteor. Soc.*, **85**, 253–277.
- [14] Weckwerth, T. M., C. Pettet, F. Fabry, S. Park, M. A. LeMone, and J. Wilson, 2005: Radar refractivity retrieval: Validation and application to short-term forecasting. *J. Appl. Meteor.*, **44**, 285–300.